Isotope Engineering of Carbon Nanotube Systems

F. Simon, Ch. Kramberger,* R. Pfeiffer, and H. Kuzmany
Institut für Materialphysik, Universität Wien, Strudlhofgasse 4, A-1090 Wien, Austria

V. Zólyomi and J. Kürti
Department of Biological Physics, Eötvös University Budapest, Pázmány Péter sétány 1/A, H-1117 Budapest, Hungary

P. M. Singer and H. Alloul
Laboratoire de Physique des Solides, UMR 8502, Université Paris-Sud, 91405 Orsay, France
(Received 15 June 2004; published 27 June 2005)

The synthesis of a unique isotope engineered system, double-wall carbon nanotubes with natural carbon outer and highly ^{13}C enriched inner walls, is reported from isotope enriched fullerenes encapsulated in single-wall carbon nanotubes (SWCNTs). The material allows the observation of the *D* line of the highly defect-free inner tubes that can be related to a curvature induced enhancement of the electron-phonon coupling. *Ab initio* calculations explain the inhomogeneous broadening of inner tube Raman modes due to the distribution of different isotopes. Nuclear magnetic resonance shows a significant contrast of the isotope enriched inner SWCNTs compared to other carbon phases and provides a macroscopic measure of the inner tube mass content. The high curvature of the small diameter inner tubes manifests in an increased distribution of the chemical shift tensor components.

DOI: 10.1103/PhysRevLett.95.017401 PACS numbers: 78.30.Na, 61.46.+w, 76.60.−k

Isotope engineering (IE) of materials provides an important degree of freedom for both fundamental studies and applications. The change in phonon energies upon isotope substitution, while leaving the electronic properties unaffected, has been used to identify vibrational modes [1–3] and gave insight into underlying fundamental mechanisms, such as phonon-mediated superconductivity [4]. Applications of IE involve, for instance, the controlled doping of isotope engineered Si heterostructures by means of neutron irradiation [5], fabrication of mononuclear devices with controlled heat conducting properties [6], and the basic architecture for spintronics and quantum computing [7]. Recently, single-wall carbon nanotubes (SWCNTs) have been intensively studied as a result of their anticipated applicability and the unique physical properties related to their quasi-one-dimensional electronic structure. Examples include the presence of Van Hove singularities in the density of states [8] and the Luttinger liquid behavior [9]. IE of carbon nanotubes using isotope enriched graphite as the starting material was attempted in order to allow NMR spectroscopy [10,11]. However, the NMR studies have been hampered by the fact that the ^{13}C NMR active nuclei can be found in all species of carbons, e.g., amorphous or graphitic carbon, inevitably present even in the purified SWCNT materials, and no nanotube selective enrichment or purification could be achieved until now. Vibrational spectroscopy is suitable to study the effect of IE. For SWCNTs, Raman spectroscopy has proven to be convenient to characterize their electronic and structural properties. In addition, Raman studies on double-wall carbon nanotubes (DWCNTs) [12,13], synthesized from fullerenes encapsulated inside the tubes (fullerene peapods) [14], provide a unique opportunity to study the small diameter inner tubes.

In this Letter, we report the preparation and study of a unique hybrid carbon nanotube material. It consists of DWCNTs where the inner tube contains ^{13}C with a controlled level of enrichment, whereas the outer tube remains natural carbon. This material is obtained by filling a host SWCNT with isotopes labeled C_{60} or C_{70} fullerenes and transforming the resulting peapods to an inner tube by high temperature annealing. Raman scattering reveals an unexpected strong response from the *D* line of the inner tubes, even though the latter are highly defect free [13]. Even at the high temperature of the peapod transformation, no exchange of carbon between the inner and outer shell is observed. The random distribution of ^{13}C atoms in the wall of the inner tube leads to a line broadening which is quantitatively explained. In contrast with nonisotope enriched tubes, the present material is an excellent object for NMR spectroscopy. This allows the measurement of the mass fraction of a material encapsulated in carbon nanotubes for the first time. The effect of high curvature is demonstrated for the small diameter inner tubes from unusual NMR line shapes.

Commercial SWCNTs (50 weight % purity, Nanocarblab, Moscow, Russia), ^{13}C isotope enriched fullerenes (MER Corp., Tucson, USA), and C_{60} of natural carbon (Hoechst AG, Frankfurt, Germany) were used to prepare fullerene peapods C_{60}, C_{70}@SWCNT. The Gaussian tube diameter distribution was determined from Raman spectroscopy [15] and revealed $d = 1.40$ nm and $\sigma = 0.10$ nm for the mean diameter and the variance, respectively. We used two grades of ^{13}C enriched fullerene mixtures: 25% and 89%, whose values are slightly refined

in our study. The 25% grade was nominally C_{60}, and the 89% grade was nominally C_{70}. For the fullerene encapsulation, the SWCNTs and the fullerenes were sealed under vacuum in a quartz ampoule and annealed at 650 °C for 2 h [16]. Fullerenes enter the SWCNTs at this temperature due to their high vapor pressure that is maintained in the sealed environment. Nonencapsulated fullerenes were removed by dynamic vacuum annealing at the same temperature. The filling of SWCNTs was characterized by high-resolution transmission electron microscopy (HR-TEM), by x-ray studies of the one-dimensional array of fullerenes inside the SWCNTs, and by the detection of the fullerene modes from the cages encapsulated inside the SWCNTs using Raman spectroscopy [16,17]. The peapods were transformed to DWCNTs by a dynamic vacuum treatment at 1250 °C for 2 h following Ref. [12]. Again, the DWCNT transformation was followed by HR-TEM and by the observation of the DWCNT structure factors with x-ray studies. In addition, new Raman modes emerge after the transformation, particularly in a frequency range that is upshifted from the outer tube radial breathing modes (RBMs). According to the $1/d$, scaling of the RBM modes, where d is the tube diameter, these lines are an additional proof for the growth of the small diameter inner shell tubes [12,13]. DWCNTs based on the fullerenes with different

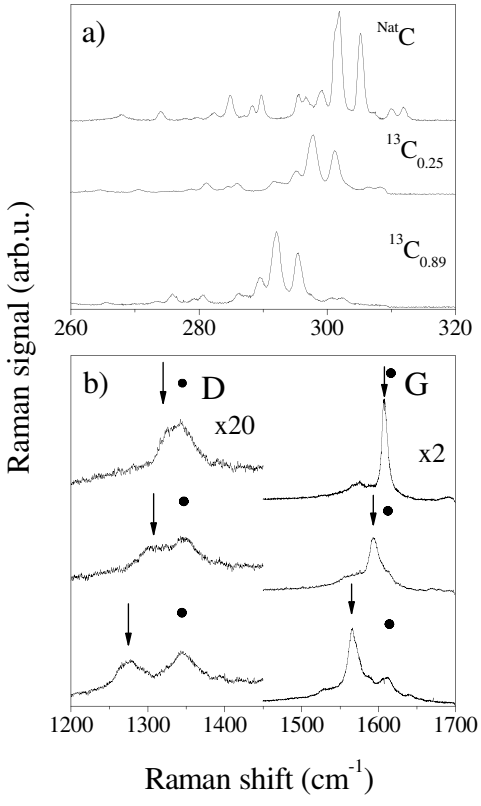

FIG. 1. Raman spectra of DWCNTs with ^{Nat}C and ^{13}C enriched inner tubes at 676 nm excitation. (a) RBM, (b) D and G mode Raman responses. Arrows and circles indicate the D and G modes of inner and outer tubes, respectively.

^{13}C enrichment grades are denoted as ^{Nat}C-, $^{13}C_{0.25}$-, and $^{13}C_{0.89}$-DWCNT. Vibrational analysis was performed on a Dilor xy triple Raman spectrometer in the 1.64–2.54 eV (676–488 nm) energy range at 90 K. The spectral resolution was 0.5–2 cm^{-1} depending on the laser wavelength and the resolution mode used. First principles calculations were performed with the Vienna *ab initio* simulation package (VASP) [18]. Magic angle spinning (MAS) and static ^{13}C-NMR spectra were measured at ambient conditions using a Chemagnets (Varian Inc.) MAS probe at 7.5 T by the Fourier transformation of the free induction decay following the excitation pulse.

In Fig. 1, we show the Raman spectra of ^{Nat}C-, $^{13}C_{0.25}$-, and $^{13}C_{0.89}$-DWCNTs for the RBMs [Fig. 1(a)], and the D and G mode spectral ranges [Fig. 1(b)] at 676 nm excitation. The narrow lines in Fig. 1(a) were identified as the RBMs of the inner tubes [13]. An overall downshift of the inner tube RBMs is observed for the ^{13}C enriched materials accompanied by a broadening. The downshift is evidence for the effective ^{13}C enrichment of inner tubes. The level of enrichment and the broadening are discussed below. The RBM lines are well separated for inner and outer tubes due to the $\nu_{\mathrm{RBM}} \propto 1/d$ relation and a mean inner tube diameter of $\sim$0.7 nm [19,20]. However, other vibrational modes, such as the defect induced D and the tangential G modes strongly overlap. Arrows in Fig. 1(b) indicate a downshifting component of the D and G modes. This component is assigned to the D and G modes of the inner tubes.

The intensities of the inner and outer tube D modes are comparable as seen in Fig. 1(b). The D mode originates from a double resonance process, which is induced by defects [21–23]. The inner tubes contain significantly less defects than the outer ones, as proven by the narrow RBM phonon linewidths [13]. Thus, the experimentally observed D band intensity suggests a competitive effect, in which the enhanced electron-phonon coupling in small diameter SWCNTs [24] compensates for the smaller number of defects.

The shift of the RBM, D, and G modes were analyzed for the two grades of enrichment. The average value of the relative shift for these modes was found to be $(\nu_0 - \nu)/\nu_0 = 0.0109(3)$ and 0.0322(3) for the ^{Nat}C-, $^{13}C_{0.25}$-, and $^{13}C_{0.89}$-DWCNTs samples, respectively. Here, ν_0 and ν are the Raman shifts of the same inner tube mode in the natural carbon and enriched materials, respectively. In a continuum model, the shift originates from the increased mass of the inner tubes. This gives $(\nu_0 - \nu)/\nu_0 = 1 - \sqrt{\frac{12+c_0}{12+c}}$, where c is the concentration of the ^{13}C enrichment on the inner tube, and $c_0 = 0.011$ is the natural abundance of ^{13}C in carbon. The resulting values of c are 0.277(7) and 0.824(8) for the 25% and 89% samples, respectively. The validity of the continuum approximation for the RBM was verified by performing *ab initio* calculations on the (5,5) tube as an example. Here, (n, m) defines the direction along which the graphene sheet is rolled up

into a tube. In the calculation, the Hessian was determined by density functional theory and the RBM frequencies were determined from the diagonalization of the dynamical matrix for a large number of random ^{13}C distributions. The distribution of the resulting RBM frequencies can be approximated by a Gaussian where center and variance give the isotope shifted RBM frequency and the spread in these frequencies. The difference between the shift determined from the continuum model and from the *ab initio* calculations is below 1%.

The broadening for the ^{13}C enriched inner tubes is best observed for the narrow RBMs. In Figs. 2(a) and 2(b) we show the RBMs of some inner tubes for the ^{Nat}C and $^{13}C_{0.25}$ samples. Figure 2(b) shows the spectrum after deconvolution with the Gaussian response of our spectrometer (curve 2). In Fig. 2(a), this is a Lorentzian, but in Fig. 2(b), the line shape still contains a Gaussian component, as discussed below. The FWHMs of the resulting line shapes are 0.76(4), 0.76(4), 0.44(4), 0.54(4), and 1.28(6), 1.30(6), 1.12(6), 1.16(6) for the inner tube RBMs shown in Fig. 2 of the ^{Nat}C and $^{13}C_{0.25}$ materials, respectively. The origin of the extra broadening is due to the random distribution of ^{12}C and ^{13}C nuclei. We found from the *ab initio* calculations for the ratio between the half width of extra broadening and the shift, $\Delta\nu/(\nu_0 - \nu)$, is $\sim$0.19 for a 30% ^{13}C enriched sample. The corresponding broadened line shapes are shown in Fig. 2(b) (curve 4). When the magnitude of the Gaussian randomness related broadening was fit (curve 3), we found that $\Delta\nu/(\nu_0 - \nu) = 0.15$. Similar broadening was observed for the 89% sample which is also reproduced by the calculation.

The current samples also allowed us to address whether carbon exchange between the inner and outer tubes occurs during the DWCNT synthesis. In Fig. 3 we compare the *G* mode spectra of ^{Nat}C- and $^{13}C_{0.89}$-DWCNTs at 488 nm excitation. For this excitation, the outer tubes dominate the spectrum since semiconducting outer and conducting inner tubes are in resonance [20]. Indeed, the only shifting component observed is small (arrows in Fig. 3) compared to the nonshifting components (circles in Fig. 3). Although the SWCNT *G* mode consists of several components [25,26], we deconvoluted the spectra with one Lorentzian line for the shifted and three Lorentzians for the nonshifted components. The nonshifted components correspond to the outer tube *G* modes and are unaffected by the ^{13}C enrichment within the 1 cm^{-1} experimental accuracy, giving an upper limit to the extra ^{13}C in the outer wall of 1.7%.

Macroscopic information about the enrichment can be obtained from NMR spectroscopy as it measures the total number of ^{13}C. In Fig. 4, we show the static and MAS spectra of ^{13}C enriched DWCNTs, and the static spectrum for the SWCNT starting material. The mass fraction belonging to the enriched phase relative to the total sample mass, *wt*, can be calculated from the integrated NMR signal by comparing it to the NMR signal of the 89% ^{13}C

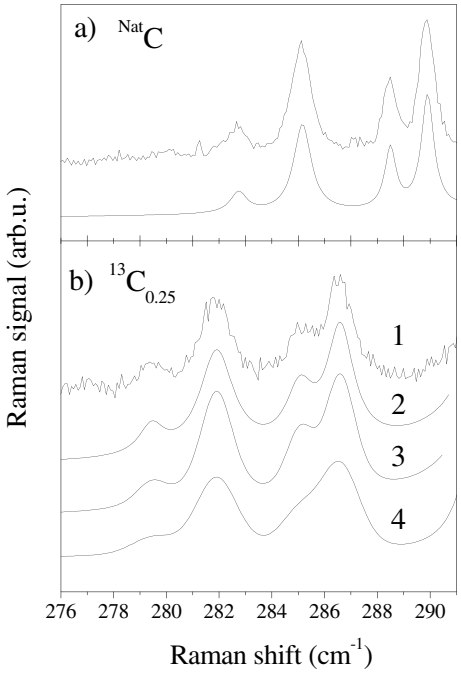

FIG. 2. RBMs of some inner tubes for 676 nm excitation with 0.5 cm^{-1} spectral resolution. (a) ^{Nat}C, (b) $^{13}C_{0.25}$. 1–4 mark the experimental spectrum, the spectrum after deconvolution by the spectrometer response, a simulated spectrum with an extra Gaussian broadening, and a calculated spectrum (see text), respectively.

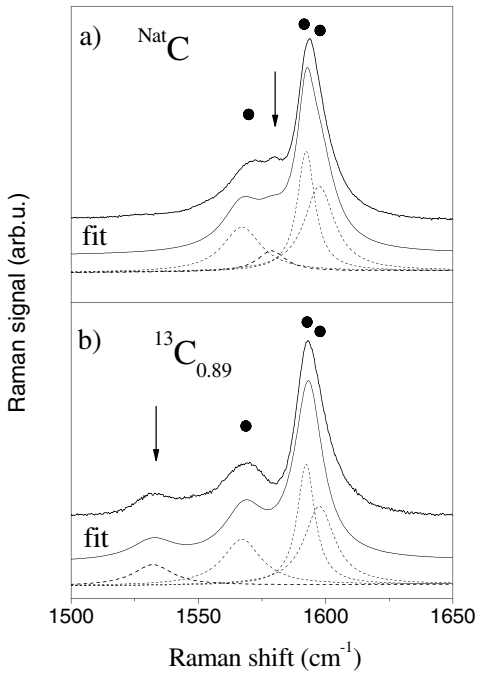

FIG. 3. *G* modes of DWCNT with ^{Nat}C (a) and 89% ^{13}C (b) enriched inner walls at 488 nm excitation. Circles and arrows indicate the nonshifting components of the outer and the shifting components of the inner tubes, respectively. Dashed curves show the deconvolution of the observed spectra.

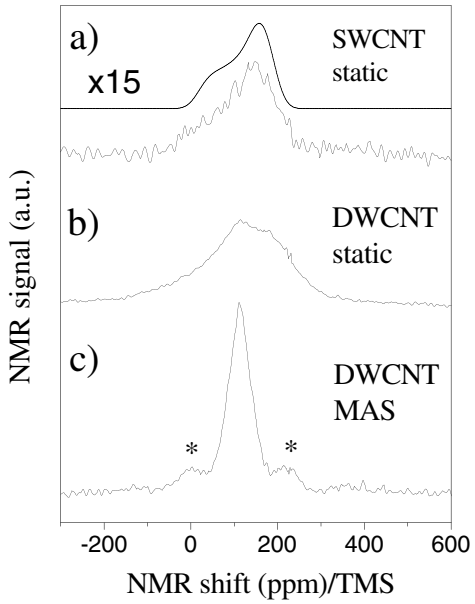

FIG. 4. NMR spectra normalized by the sample mass, taken with respect to tetramethylsilane (TMS) shift: (a) static spectrum for nonenriched SWCNT enlarged by a factor of 15, (b) static, and (c) MAS spectra of $^{13}C_{0.89}$-DWCNT. Smooth curve is a CSA powder pattern simulated with literature parameters [10]. Asterisks show the spinning sidebands at 8 kHz.

enriched fullerene, and we found $wt = 13(4)\%$. The expected mass ratio of inner tubes as compared to the total sample mass is 15%, which is obtained from the SWCNT purity (50%), ~70% volume filling in highly filled peapod samples [27], and the mass ratio of encapsulated fullerenes to the mass of the SWCNTs. The measured mass fraction of the highly enriched phase is very similar to that of the calculated mass fraction of inner tubes. This suggests that the NMR signal comes nominally from the inner tubes, and other carbon phases such as amorphous or graphitic carbon are not ^{13}C enriched.

The typical chemical shift anisotropy (CSA) powder pattern is observed for the SWCNT sample in agreement with previous reports [10,11]. However, the static DWCNT spectrum cannot be explained with a CSA powder pattern. The complicated structure of the spectrum suggests that the chemical shift tensor parameters are distributed for the inner tubes. It is the result of the higher curvature of inner tubes as compared to the outer ones: the variance of the diameter distribution is the same for the inner and outer tubes [20] but the corresponding bonding angles show a larger variation [28]. In addition, the residual linewidth in the MAS experiment, which is a measure of the sample inhomogeneity, is 60(3) ppm, i.e., about twice as large as the ~35 ppm found previously for SWCNT samples [10,11]. The isotropic line position, determined from the MAS measurement, is 111(2) ppm. This value is significantly smaller than the isotropic shift of the SWCNT samples of 125 ppm [10,11], which might originate from different C-C bonding angles of the inner tubes, or from diamagnetic shielding of the outer tubes.

In conclusion, we report on the synthesis of ^{13}C enriched inner tubes embedded inside a natural carbon outer tube. The ^{13}C enriched inner tubes facilitate the identification of the vibrational modes of inner and outer tubes. ^{13}C only resides in the inner shell of the DWCNTs, without enriching other carbon phases such as the inevitable amorphous carbon or graphite, which simplifies the analysis of NMR experiments where nanotube sensitive information is desired. The described isotope engineering may find application for the controllable doping of SWCNTs, similar to the isotope engineering applied in the Si semiconducting industry.

We thank H. Peterlik for the x-ray studies. Work supported by the FWF 14893, OTKA T038014, and EU BIN2-2001-00580, MEIF-CT-2003-501099, and HPMF-CT-2002-02124 projects. Calculations were performed on the Schrödinger II cluster at the University of Vienna. F. S. acknowledges the Zoltán Magyary program for support.

*Present address: Leibniz-Institut für Festkörper- und Werkstoffforschung, D-01069, Dresden, Germany.

[1] M. C. Martin *et al.*, Phys. Rev. B **51**, 2844 (1995).
[2] A. Rosenberg and C. Kendziora, Phys. Rev. B**51**, 9321 (1995).
[3] P. J. Horoyski *et al.*, Phys. Rev. B **54**, 920 (1996).
[4] J. Bardeen, L. N. Cooper, and J. R. Schrieffer, Phys. Rev. **108**, 1175 (1957).
[5] *Neutron Transmutation Doping of Semiconductors*, edited by J. Meese (Plenum, New York, 1979).
[6] W. S. Capinski *et al.*, Appl. Phys. Lett. **71**, 2109 (1997).
[7] I. Shlimak, cond-mat/0403421.
[8] M. S. Dresselhaus, G. Dresselhaus, and P. C. Eklund *Science of Fullerenes and Carbon Nanotubes* (Academic, San Diego, 1996).
[9] H. Ishii *et al.*, Nature (London) **426**, 540 (2003).
[10] X.-P. Tang *et al.*, Science **288**, 492 (2000).
[11] C. Goze-Bac *et al.*, Carbon **40**, 1825 (2002).
[12] S. Bandow *et al.*, Chem. Phys. Lett. **337**, 48 (2001).
[13] R. Pfeiffer *et al.*, Phys. Rev. Lett. **90**, 225501 (2003).
[14] B. W. Smith *et al.*, Nature (London) **396**, 323 (1998).
[15] H. Kuzmany *et al.*, Eur. Phys. J. B **22**, 307 (2001).
[16] H. Kataura *et al.*, Synth. Met. **121**, 1195 (2001).
[17] T. Pichler *et al.*, Phys. Rev. Lett. **87**, 267401 (2001).
[18] G. Kresse and D. Joubert, Phys. Rev. B **59**, 1758 (1999).
[19] M. Abe *et al.*, Phys. Rev. B **68**, 041405 (2003).
[20] F. Simon *et al.*, cond-mat/0404110.
[21] C. Thomsen and S. Reich, Phys. Rev. Lett. **85**, 5214 (2000).
[22] J. Kürti *et al.*, Phys. Rev. B **65**, 165433 (2002).
[23] V. Zólyomi *et al.*, Phys. Rev. Lett. **90**, 157401 (2003).
[24] L. X. Benedict *et al.*, Phys. Rev. B **52**, 14 935 (1995).
[25] M. A. Pimenta *et al.*, Phys. Rev. B **58**, R16016 (1998).
[26] O. Dubay *et al.*, Phys. Rev. Lett. **88**, 235506 (2002).
[27] X. Liu *et al.*, Phys. Rev. B **65**, 045419 (2002).
[28] J. Kürti *et al.*, New J. Phys. **5**, 125 (2003).